Journal of the Korean Chemical Society
2023, *Vol. 67, No. 6*
Printed in the Republic of Korea
https://doi.org/10.5012/jkcs.2023.67.6.407

Vibrational Relaxation and Bond Dissociation in Methylpyrazine on Collision with N_2 and O_2

Young-Jin Yu, Sang Kwon Lee*, and Jongbaik Ree*
Department of Chemistry Education, Chonnam National University, Gwangju 61186, Korea.
**E-mail: lsk1213@jnu.ac.kr; jbree@jnu.ac.kr*
(Received September 18, 2023; Accepted October 13, 2023)

ABSTRACT. The present study uses quasi-classical trajectory procedures to examine the vibrational relaxation and dissociation of the methyl and ring C–H bonds in excited methylpyrazine (MP) during collision with either N_2 or O_2. The energy-loss ($-\Delta E$) of the excited MP is calculated as the total vibrational energy (E_T) of MP is increased in the range of 5,000 to 40,000cm $^{-1}$. The results indicate that the collision-induced vibrational relaxation of MP is not large, increasing gradually with increasing E_T between 5,000 and 30,000 cm^{-1}, but then decreasing with the further increase in E_T. In both N_2 and O_2 collisions, the vibrational relaxation of MP occurs mainly via the vibration-to-translation ($V \rightarrow T$) and vibration-to-vibration ($V \rightarrow V$) energy transfer pathways, while the vibration-to-rotation ($V \rightarrow R$) energy transfer pathway is negligible. In both collision systems, the $V \rightarrow T$ transfer shows a similar pattern and amount of energy loss in the E_T range of 5,000 to 40,000cm^{-1}, whereas the pattern and amount of energy transfer via the $V \rightarrow V$ pathway differs significantly between two collision systems. The collision-induced dissociation of the C–H_{methyl} or C–H_{ring} bond occurs when highly excited MP (65,000–72,000 cm^{-1}) interacts with the ground-state N_2 or O_2. Here, the dissociation probability is low (10^{-4}–10^{-1}), but increases exponentially with increasing vibrational excitation. This can be interpreted as the intermolecular interaction below E_T = 71,000 cm^{-1}. By contrast, the bond dissociation above E_T = 71,000 cm^{-1} is due to the intramolecular energy flow between the excited C–H bonds. The probability of C–H_{methyl} dissociation is higher than that of C–H_{ring} dissociation.

Key words: Collision-induced, Quasi-classical, Methylpyrazine, Energy transfer

INTRODUCTION

The vibrational energy transfer of excited diatomic and polyatomic molecules is essential for understanding the elementary processes that play crucial roles in chemical reactions.[1-11] In particular, the collision-induced relaxation of vibrationally excited diatomic and polyatomic molecules is of specific interest as it directly affects the nature of bond dissociation and subsequent chemical reaction dynamics. Such excitation can be examined directly by using various experimental techniques such as time-resolved infrared laser excitation[12-14] or electronic-impact excitation,[15,16] or indirectly via intramolecular vibrational energy redistribution (IVR).[17]

Several studies have reported on the collision-induced vibrational energy flow of various excited large organic molecules.[7,9-12,18-19] Among those, toluene and its derivatives are especially attractive for investigating collision-induced vibrational relaxation and bond dissociation during collisions with atoms or molecules. For example, Hippler *et al.* studied the collision-induced vibrational relaxation of excited toluene via collisions with ~60 different atoms and molecules,[19] while Toselli *et al.* reported the collision-induced vibrational relaxation of excited toluene due to 20 colliders by monitoring the time-resolved infrared fluorescence (TR-IRF) absorbances of the methyl C–H and ring C–H bonds near 3.3 mm.[20] Meanwhile, computational studies on the collision-induced energy transfer between large organic molecules have been reported by Bernshtein and Oref.[21]

On the other hand, methylpyrazine (MP) is a particularly interesting molecule because while it contains C–C bonds as toluene, this also include two distinct types, namely the methyl C–H bonds and the ring C–H bonds. Collisions between these bonds and other atoms or molecules can lead to the flow of both intermolecular and intramolecular energy from one C–H bond to another via the C–C bonds.[22] Hence, the present paper is aimed at examining the collision-induced dynamics of vibrationally excited MP upon interaction with N_2 and O_2 by using quasi-classical trajectory calculations. When the molecule is vibrationally excited, the important considerations are the determination of energy transfer as a function of vibrational excitation and the extent of bond dissociation on collision. The first of these involves the intermolecular energy transfer between the incident particle and MP, which occurs via

vibration-to-translation ($V \rightarrow T$) and vibration-to-vibration ($V \rightarrow V$) transfer, and intramolecular energy flow, which occurs via vibration-to-vibration ($V \rightarrow V$) energy transfer between stretching and bending vibrations. When the total energy content (E_T) is sufficiently high, either the ring C–H or the methyl C–H can dissociate, and the efficiency of each bond dissociation depends upon the amount and distribution of the initial vibrational excitation. Hence, the calculation results are used to discuss the relaxation and dissociation of the excited C–H vibrations, and compare and contrast them in both the N_2 and O_2 collision systems.

INTERACTION MODEL AND ENERGIES

The collision-induced dynamics in MP are investigated herein by using the same model as that developed for the reaction between toluene and N_2 or O_2.[23] The interaction model for the reaction of MP with N_2 is shown schematically in *Fig.* 1, where both species are located in the same plane, and the stretching and bending coordinates of MP are indicated, along with the vibrational and rotational coordinates of N_2. The reaction system consists of the interaction zone, where the colliding molecule interacts with both the methyl and ring C–H bonds (C–H_{methyl} and C–H_{ring}), and the inner zone, which includes the various stretching and bending vibrations of MP. To formulate the interaction energies between MP and the N_2 molecule, the interatomic distances r_1-r_4 are expressed in terms of the coordinates of the C–H_m bond, the C–CH_3 bond, the (C–C)$_r$ bond, the C–H_r bond, the C–C–H_m bending group, the C–C–CH_3 bending group, the C–C–H_r bending group (where the subscripts m and r represent methyl and ring, respectively), and the vibrational and rotational coordinates of the incident N_2 molecule. In other words, r_i (where $i = 1$, 2, 3, or 4) is expressed as r_i (z, x_1, x_2, x_3, x_4, ϕ_1, ϕ_2, ϕ_5, x, h, h', Ξ), where z is the distance between the center of mass of MP and that of N_2, x indicates a stretching vibration, ϕ indicates a bending vibration, ξ is the displacement of N_2 from its equilibrium bond distance, η and η' are the rotational angles of N_2, and Ξ is the incident angle.

The various parameters for MP, including the dissociation energy (D_{oi}), bond distance (d_i), frequency (ν_i), bending angle, and bending frequency, are summarized in *Table* 1. Here, the *ab initio* calculations for obtaining those parameters in MP were performed using the GAUSSIAN 2016 software, and the range parameters were determined using the relation $b_i = (2D_i/\mu_i)^{1/2}/\omega_i$, where ω_i is $2\pi\nu_i$ and $D_i = D_{oi} + \frac{1}{2}\hbar\omega_{ei}$, where ω_{ei} is $2\pi\nu_{ei}$ and $\hbar$ is Planck's constant divided by 2π.

The $N_{(1)}$-to-H_r, $N_{(1)}$-to-H_m, $N_{(2)}$-to-H_r, and $N_{(2)}$-to-H_m distances (r_1–r_4) and associated interatomic distances can be derived by using the trigonometrical functions.[23] The overall interaction energy (V) between MP and N_2 (or O_2) is expressed by Eq. (1):

$$V = \sum U(r_k) + U_s(x_i) + U_b(\phi_j) + U_{int}(Y_i Y_j) + U_{inc}(\xi, \rho, \rho') + \frac{-3I_1I_2}{2(I_1+I_2)}\frac{\alpha_1\alpha_2}{z^6} \quad (1)$$

where $U(r_k)$, $U_s(x_i)$, $U_b(\phi_j)$, $U_{int}(Y_iY_j)$ and $U_{inc}(\xi, \rho, \rho')$ represent the Morse-type intermolecular terms, Morse-type stretching terms and the harmonic bending terms of MP, and intramolecular coupling terms in MP, respectively, and the last term represents the London interaction.[23] Also, I_i is the ionization potential, α_i is the polarizability, and the subscripts s and b represent the stretching and bending vibrations, respectively, and *int* represent the interaction between and stretching and bending vibrations, and *inc*

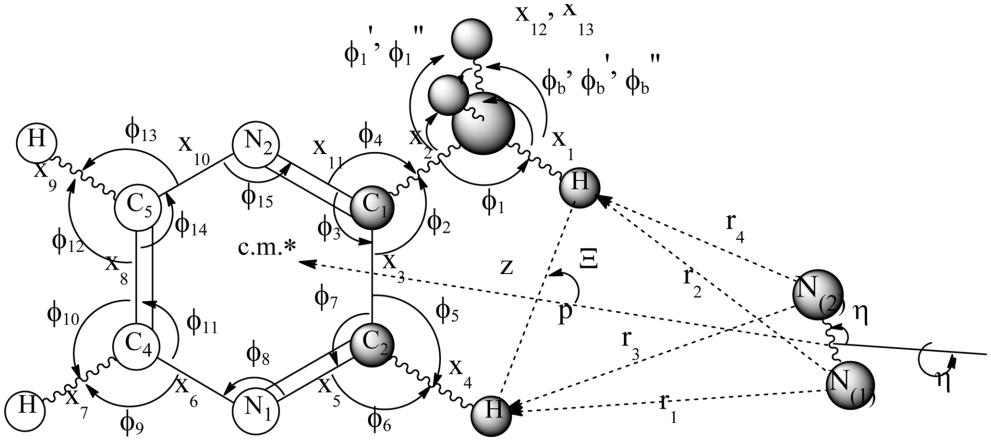

***Figure* 1.** The collision model for MP + N_2, where all the C and N atoms are considered to lie in the same plane.

***Table* 1.** The molecular parameters for methylpyrazine

Stretches	C–H $i=1$	C–H $i=4$	C–H $i=7$	C–H $i=9$	C–H $i=12,13$	C–C $i=3$	C–C $i=8$	C–CH_3 $i=2$	C–N $i=5,6,10,11$
Dissociation energy, D_{oi}(eV)[a]	4.123	4.804	4.809	4.849	4.123	5.308	5.638	4.273	7.121
Bond distance, d_i(Å)[a]	1.091	1.086	1.085	1.086	1.093	1.401	1.393	1.503	1.333
Frequency, ν_i(cm^{-1})[a]	3114[c]	3151[c]	3168[c]	3168[c]	3093[c]	1219[c]	1613[c]	1268[d]	1219[c]
Range parameter, b_i(Å)	0.496	0.532	0.529	0.532	0.499	0.569	0.425	0.465	0.622
Bends	φ_1, φ_1', φ_1''	φ_2	φ_3	ϕ_4	ϕ_5	ϕ_6	ϕ_7	ϕ_8	ϕ_9
Bond angle (°)	111.6	122.1	120.2	117.6	120.5	116.7	122.7	116.3	117.3
Frequency, ν_i(cm^{-1})	1506	349	566	349	1426	1327	647	1309	1202
Bends	ϕ_{10}	ϕ_{11}	ϕ_{12}	ϕ_{13}	ϕ_{14}	ϕ_{15}	$\phi_b\phi_b'$,ϕ_b''	–	–
Bond angle (°)	121.1	121.4	120.9	117.0	122.0	117.1	108.7	–	–
Frequency, ν_i(cm^{-1})	1202	841	1327	1327	647	566	1477	–	–

represent the incident molecule (N_2 or O_2). The Lennard–Jones (LJ) parameters for each reaction were determined by applying the combining rules,[24] with $a = 0.372$ and 0.365 Å for MP + N_2 and MP + O_2, respectively.[24,25] Here, the values of $\varepsilon = 247k_B$ and $\sigma = 4.640$ Å were used for the MP + N_2 reaction, and $\varepsilon = 274k_B$ and $\sigma = 4.516$ Å for the MP + O_2 reaction.

The molecular constants for the MP, N_2, and O_2, including the ionization energy, polarizability, dissociation energy, frequency, bond distance, and range parameter are listed in *Table* 2.[25-27] The dissociation energies, bond distances, and vibrational frequencies of N_2 and O_2 were computed at the B3LYP/6-311+G(d,p) level of theory.

The equations of motion for monitoring the time dependence of the collision trajectory and the interaction motions can be written as Eq. (2):

$$M_k d^2q_k(t)/dt^2 = -\partial V(z, x_1\text{–}x_{13}, \phi_1\text{–}\phi_{20}, \xi, \eta, \eta')/\partial q_k;\quad k = A, B, C, \xi, \eta, \text{ or } \eta' \qquad (2)$$

where $k = A$ represents the collision trajectory with the reduced mass $M_A = \mu$; $k = B$ represents the stretching vibrational modes x_1–x_{13} with the associated mass $M_B = \mu_I$; $k = C$ represents the bending vibrational modes ϕ_1–ϕ_{20} with the associated moment of inertia $M_C = I_j$; for the incident molecule (e.g., N_2), $k = \xi$ represents the vibration with the reduced mass $M_\xi = \mu_{inc}$, and $k = \eta$ and η' represent the rotations with the associated moment of inertia $M_\eta = I_{inc}$. These equations and their associated conjugate quantities $dr(t_o)/dt$, $dx_i(t_o)/dt$, $d\phi_j(t_o)/dt$, $d\xi(t_o)/dt$, $d\eta(t_o)/dt$, and $d\eta'(t_o)/dt$ were integrated for each initial condition by using the standard numerical routines.[28,29] A total of 100,000 trajectories were sampled for each vibrationally excited state of MP, and the collision energies (E) were sampled from the Maxwell distributions at 300 K. Also, for each trajectory, the initial rotational energy of N_2 or O_2 was selected from the quantum-mechanical correspondence $p_q = [J(J+1)]^{1/2}\hbar$, where J was sampled from $(2J+1)\exp[-J(J+1)\hbar^2/2k_BT]/Q_r$, where Q_r is the rotational partition function. Meanwhile, the vibrational energy of N_2 or O_2 was fixed at $v = 0$, 1, or 2 to observe the energy loss of MP by collision with N_2 or O_2 in the vibrational ground and excited states. Thus, each trajectory enters the reaction channel with well-defined vibrational and rotational energies at 300 K. The initial conditions for the collision trajectory, and the relative vibrational and rotational motions for solving the equations of motion, are given elsewhere.[30] The ensemble-averaged energy loss in the vibrationally excited MP was calculated as the difference between the final and initial energies of the reaction partner, that is, $-\Delta E = E_{initial} - E_{final}$.

***Table* 2.** The molecular constants for MP, N_2, and O_2

Molecule	MP	N_2	O_2
Ionization energy, I_i (eV)	8.828[a]	15.581[b]	12.0697[b]
Polarizability, α_i (Å^3)	9.045[b]	1.710[c]	1.562[c]
Dissociation energy, D_{oi} (eV)[d]	–	9.749	5.640
Frequency, ν_i (cm^{-1})[d]	–	2445	1634
Bond distance, d_i (Å)[d]	–	1.096	1.206
Range parameter, b_i (Å)[e]	–	0.356	0.379

[a]Ref. 26
[b]Ref. 25
[c]Ref. 27
[d]B3LYP/6-311+G(d,p) level *ab initio* calculation.
[e]Determined from the relation $b_i = (2D_{oi}/\mu_i)^{1/2}/\omega_i$.

RESULTS AND DISCUSSION

The dependence of the ensemble-averaged energy loss ($-\Delta E$) of MP on the total energy (E_T) of MP in the MP + N_2 collision is shown in *Fig*. 2. Specifically, the energy losses are analyzed in terms of vibration-translation ($V \rightarrow T$), vibration-vibration ($V \rightarrow V$), and vibration-rotation ($V \rightarrow R$) processes in *Fig*. 2(a). Here, N_2 is considered to be in the

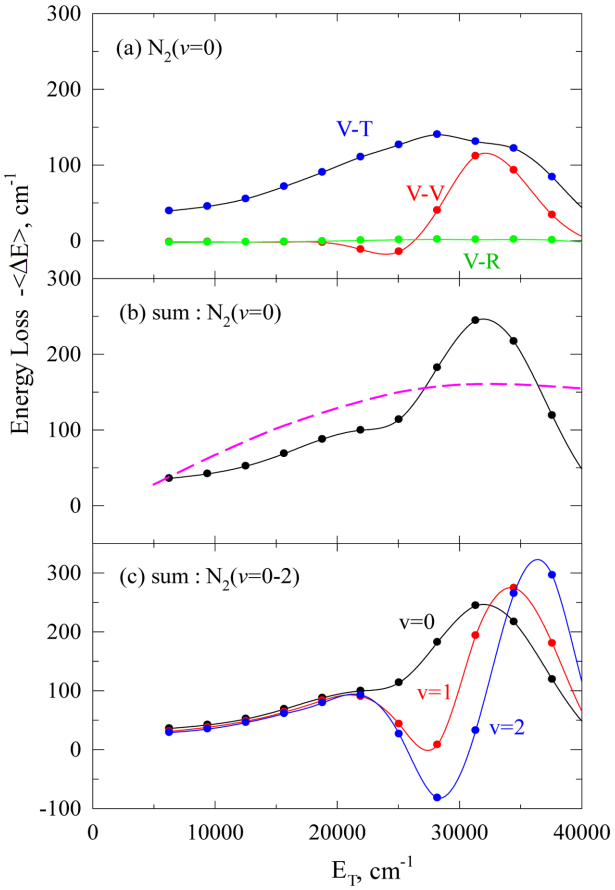

***Figure* 2.** The energy loss of MP upon collision with N_2 *vs*. the initial excitation energy of MP: (a) the individual $V \rightarrow V$, $V \rightarrow T$, and $V \rightarrow R$ transfers from MP to N_2 (v = 0); (b) the sum of all three contributions in (a). Dashed line: the experimental data for the *toluene* + N_2 collision (Ref. 31)., and (c) the dependence of the sum on the N_2 vibrational state (v = 0–2).

vibrational ground state (N_2(v=0)), and $V \rightarrow T$ means the initial excited vibrational energy of the MP is transferred to the translational energy of the collision partner (N_2). At the lowest value of E_T (6265 cm^{-1}), which corresponds to the total vibrationally excited energy of the C–H_r (3151 cm^{-1}) and C–H_m (3114 cm^{-1}) bonds, the energy loss is 36 cm^{-1}, which is obtained as the sum of 39, –1, and –2 cm^{-1} (representing the $V \rightarrow T$, $V \rightarrow V$, and $V \rightarrow R$ pathways, respectively). When E_T is increased to 31,320 cm^{-1} (i.e., the C–H_r energy is 15,750 cm^{-1} and C–H_m vibrational energy is 15,570 cm^{-1}), the total energy loss is 244 cm^{-1}, which is still less than 1% of the excited energy of MP.

The results in *Fig*. 2(a) indicate that the $V \rightarrow T$ and $V \rightarrow V$ processes are both important in the vibrational relaxation of MP in the MP + N_2 collision system, whereas the contribution of the $V \rightarrow R$ process is insignificant over the entire considered E_T range. The contribution of the $V \rightarrow T$ process gradually increases from 39 cm^{-1} at E_T = 6265 cm^{-1} to 140 cm^{-1} at E_T = 28,190 cm^{-1}, but then decreases to 84 cm^{-1} at E_T ~ 37,600 cm^{-1}. At the same time, the $V \rightarrow R$ value varies by less than ±2 cm^{-1}, while the $V \rightarrow V$ pathway exhibits a highly structured variation over the considered E_T range. Specifically, the $V \rightarrow V$ energy transfer is less than ±15 cm^{-1} until E_T = 27,000 cm^{-1}, but rapidly increases to 112 cm^{-1} at E_T = 32,300 cm^{-1}. However, it is important to note that this quasi-classical method presents limitations that make it difficult to predict the vibrational quantum effects such as quantum mechanical tunneling. Nevertheless, the ensemble-averaged $V \rightarrow V$, $V \rightarrow T$, and $V \rightarrow R$ values calculated by the quasiclassical method are highly valuable because each pathway can be elucidated effectively.

The sum of all three processes is shown in *Fig*. 2(b). Here, as E_T is increased from 6265 to 31,300 cm^{-1}, the sum increases gradually from 36 to 244 cm^{-1}. With the further increase in E_T, however, the energy loss decreases to reach 50 cm^{-1} at E_T = 40,000 cm^{-1}. Since experimental data on the MP + N_2 system are presently unavailable, the present calculation results are compared with the experimental data for the toluene + N_2 system over the considered E_T range, as reported by Wright *et al*.[31] Here, the calculated MP energy loss is comparable with their data between 5000 cm^{-1} and 40000 cm^{-1}, furthermore, they also showed the appearance of a weak maximum over the considered range of E_T.[31] Notably, a similar appearance in the vibrational relaxation of MP relative to that of toluene has also been reported in the a-chlorotoluene (a-CT) + N_2 or O_2 collision systems by Lee *et al*.[32] Moreover, the latter group also showed the appearance of a maximum in the energy loss over the considered E_T range. This trend is consistent with the well-known behavior of the vibrational relaxations of toluene and its derivatives via collisions with diatomic molecules.[31,33]

While the C–H_r vibrational relaxation remains negligible regardless of the amount of initial excitation of the C–H_r bond during the collision-induced vibrational relaxation of MP by N_2, the amount of C–H_m vibrational decay increases moderately as the initial excitation of the C–H_m bond vibrational energy increases. Due to the collision, the C–H_m vibrational energy is decreased from an initial 14,180 cm^{-1} to a final 13,348 cm^{-1}, thus implying that the amount of C–H_m vibrational decay is 832 cm^{-1}. In this case, the colliding N_2 gains 172 and 368 cm^{-1} through the $V \rightarrow T$ and $V \rightarrow V$ intermolecular processes, respectively, and the remaining energy is transferred to the $(C–C)_r$ bond, the C–CH_2–H_m bending vibration, and the C–C–CH_3 bending vibration via the intramolecular $V \rightarrow V$ pro-

cess. However, when the initial C–H_r vibrational energy is 14,013 cm^{-1}, the magnitude of the C–H_r vibrational decay via collision is only 78 cm^{-1}. Therefore, the vibrational relaxation of MP takes place primarily through the C–H_m vibrational decay. Moreover, the results of previous studies indicate that the methyl group bonded to the benzene ring is more effective than that bonded to the side chain at transferring the initial vibrational excitation to the internal N–H stretching mode.[12]

For a complete analysis of the relaxation process for MP, the energy losses due to the vibrational, rotational, and translational modes under various vibrational states of the colliding molecule (N_2) must be considered along with those of the ground state. Thus, the energy losses ($-\Delta E$) of MP for the v = 0, v = 1, and v = 2 vibrational excited states of N_2 are presented together in *Fig.* 2(b). Here, clear differences in the energy loss of MP are observed as the vibrational state of N_2 increases from 0 to 1 to 2. The $V \rightarrow V$ value for N_2 (v = 1) decreases rapidly from –7 cm^{-1} at E_T = 6265 cm^{-1} to –136 cm^{-1} at E_T = 28,200 cm^{-1}, and to 150 cm^{-1} at E_T = 34,500 cm^{-1}, whereas the $V \rightarrow T$ and $V \rightarrow R$ values are nearly the same as those for N_2 (v = 0). Thus, this variation in $-\Delta E$ of MP for N_2 (v = 1) is mainly due to the $V \rightarrow V$ process. Further, the energy loss of MP in collision with the N_2 (v = 2) state is similar to, but more rapid than, that observed for the N_2(v =1) state. Due to the similarity, the energy loss for N_2 (v = 2) is also attributed to the $V \rightarrow V$ process. For E_T = 6265 cm^{-1}, which corresponds to the sum of the initial energies of C–H_m (3151 cm^{-1}) and C–H_r (3114 cm^{-1}), the C–H_m frequency estimated by the Fourier transform is 2895 cm^{-1}. By contrast, the vibrational frequencies of N_2(v) for v = 0, 1, and 2 are 2414, 2379, and 2344 cm^{-1}, respectively, which are not close to the C–H_m frequency at E_T = 6265 cm^{-1}; thus, the $V \rightarrow V$ value is low at this E_T. However, as the E_T increases to 28,200 cm^{-1}, the estimated C–H_m frequency decreases to 2356 cm^{-1}, which is close to the vibrational frequency of N_2(v). Because the $V \rightarrow V$ energy mismatch decreases as the vibrational state of N_2 increases, the $V \rightarrow V$ value also increases; thus, the sum total energy loss of MP shows a large variation (*Fig.* 2(c)).

On the other hand, it should be interesting to note frequency changes in the before and after collision, thus we considered a typical single trajectory for MP + N_2 collision system. For this trajectory, MP transfers 0.0246 and 0.0124 eV to N_2 via $V \rightarrow T$ and $V \rightarrow V$ energy transfer, respectively. *Fig.* 3 shows the power spectrum obtained from the Fourier transform of the C-H vibrations in the excited MP. In *Fig.* 3(a), two peaks of C-H_r vibration are appearing at 2343 and 2296 cm^{-1}, reflecting the before and after collision frequencies of highly excited C-H_r vibration, respectively. The before collision frequency 2343 cm^{-1} is close to 2358 cm^{-1}, the frequency of the incident N_2 molecule, thus C-H_r can be perturbed effectively by the incident N_2 molecule. Upon collision with N_2, the C-H_r bond gained 0.100 eV in this typical case, thus the C-H_r bond starts out the collision process with the frequencies 2343 cm^{-1}, but the C-H_r vibration slightly excited to the state with the frequency 2296 cm^{-1} at the end of collision. On the contrary, the C-H_m bond lost 0.216 eV upon collision with N_2, thus, as shown in *Fig.* 3(b), the C-H_m bond starts out the collision process with the frequencies 2167 cm^{-1}, but the C-H_m vibration relaxes to the state with the frequency 2279 cm^{-1} at the end of collision.

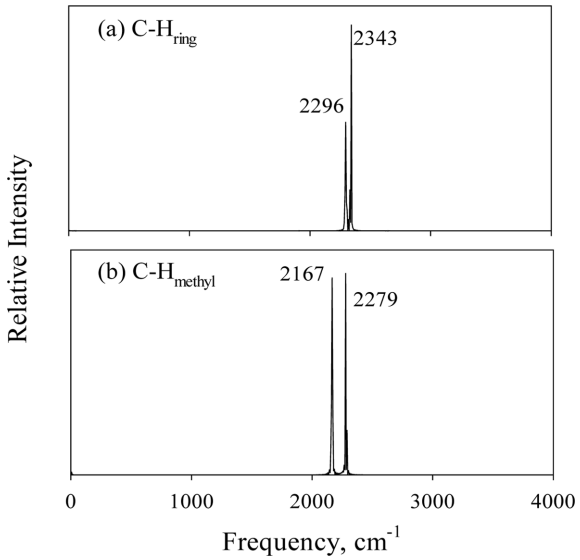

***Figure* 3.** Power spectrum obtained from the C-H_{ring} and C-H_{methyl} vibrations in MP for the typical single trajectory.

While the mass of the O_2 molecule is slightly greater than that of N_2, its vibrational frequency is significantly lower. The relationship between $-\Delta E$ and E_T in the MP + O_2 collision system is shown in *Fig.* 4. Here, the $V \rightarrow V$ value varies from 5 to 42 cm^{-1} over the considered E_T range, while the variation in $V \rightarrow R$ is negligible (±3 cm^{-1}) (*Fig.* 4(a)). However, the $V \rightarrow T$ value varies significantly from 46 to 158 cm^{-1}, thus providing the main contribution to the energy transfer between MP and O_2 (v=0). The total energy loss of MP for each vibrational state of O_2 (v = 0, 1, and 2) is shown in *Fig.* 4(b). Thus, at v = 0, the total energy loss increases gradually from 49 to 177 cm^{-1} as E_T is increased from 6265 to 28,200 cm^{-1}. However, the energy losses of MP for O_2 (v =1) and O_2 (v = 2) are seen to increase with increasing vibrational excitation of O_2 over the consid-

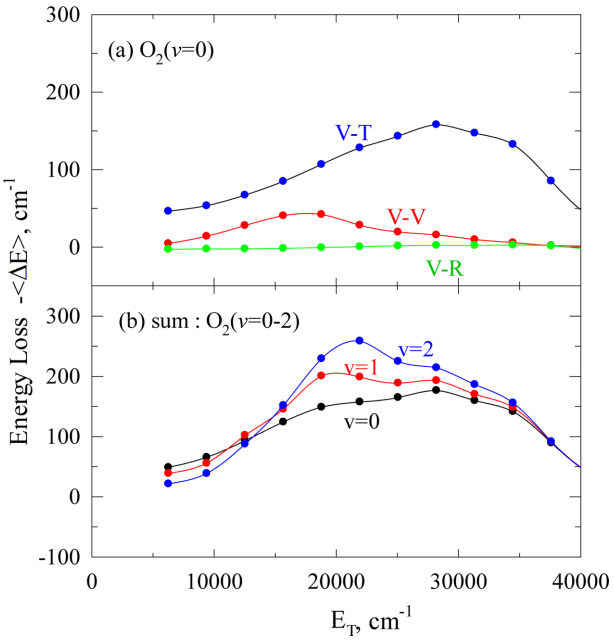

***Figure* 4.** The energy loss of MP during collision with O_2 vs. the initial excitation energy of MP: (a) the individual $V\rightarrow V$, $V\rightarrow T$, and $V\rightarrow R$ transfers from MP to O_2 (v = 0), and (b) the total energy losses depending on the O_2 vibrational state (v = 0–2).

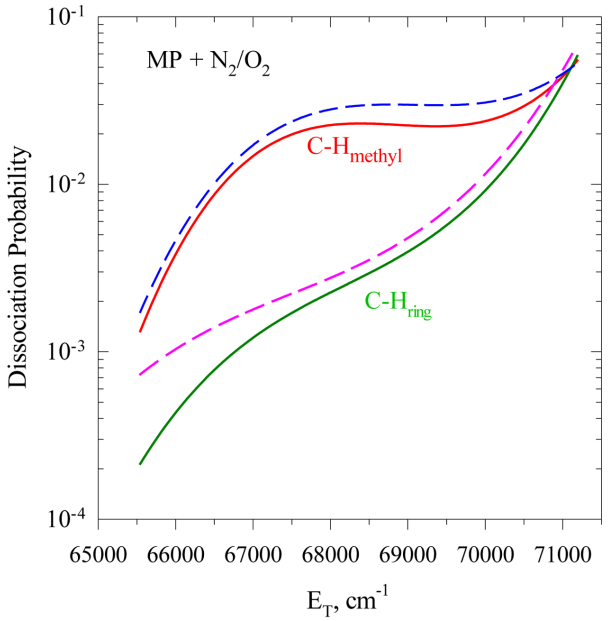

***Figure* 5.** The dissociation probabilities for the C–H_m and C–H_r bonds during the MP + N_2 collision (solid lines; red = C–H_m, green = C–H_r) and the MP + O_2 collision (dashed lines; blue = C–H_m, pink = C–H_r).

ered E_T range. This increase in energy loss is mainly caused by the $V\rightarrow V$ energy transfer. For E_T = 21,930 cm^{-1}, which corresponds to the sum of the initial input energies of the C–H_m bond (11,030 cm^{-1}) and the C–H_r bond (10,900 cm^{-1}), the $V\rightarrow V$ value is seen to increase from 28, through 69, to 128 cm^{-1} as the vibrational state of $O_2(v)$ is increased from 0 to 1 to 2, respectively. For the initial energy of the C–H_m bond (11,030 cm^{-1}), the estimated C–H_m frequency is 2543 cm^{-1}, whereas the vibrational frequencies of $O_2(v)$ for v = 0, 1, and 2 are 1611, 1587, and 1552 cm^{-1}, respectively, which are not close to the estimated C–H_m frequency at E_T = 21,930 cm^{-1}. However, the overtone frequency of $O_2(v)$ becomes closer to the estimated C–H_m frequency as the vibrational excitation state of O_2 is increased. Therefore, the $V\rightarrow V$ energy transfer increases as the vibrational excitation of $O_2(v)$ is increased.

When MP is sufficiently excited, either the C–H_r or C–H_m bond can be dissociated via collision. The semilogarithmic plots in *Fig.* 5 indicate the dissociation probabilities of the C–H_r and C–H_m bonds in the MP + N_2 reaction (solid lines) and the MP + O_2 reaction (dashed lines) at 300 K. Here, the dissociation probabilities for both systems are seen to be very low (~10^{-5}) below E_T = 65,000 cm^{-1}, but rapidly increase with increasing excitation of MP. Both dissociation probabilities are seen to be as high as ~0.05 at E_T = 71,188 cm^{-1}, in which each C-H bond energy is 0.05 eV below the threshold.

In the case of the MP + N_2 system, the C–H_r and C–H_m bond dissociations both begin when the total excitation energy is above E_T = 65,500 cm^{-1} (*Fig.* 5). Here, the dissociation probability of the C–H_r bond (green solid line) is lower than that of the C–H_m bond (red solid line) at an E_T of slightly under 71,000 cm^{-1}. However, the dissociation probability of the C–H_r bond is higher than that of the C–H_m bond above E_T = 71,000 cm^{-1}. The energy of the C–H_r or C–H_m bond has to reach the energy threshold to facilitate the dissociation of each bond via intermolecular or intramolecular interactions. At an E_T of less than 71,000 cm^{-1}, these bond dissociations occur mainly via the intermolecular interactions. Therefore, the dissociation probability of the C–H_m bond is higher than that of C–H_r bond because the perturbation of the C–H_m bond by the collision is more efficient than that of the C–H_r bond. However, the *intra*molecular interaction becomes more efficient when the total excitation of MP increases to 71,000 cm^{-1}. In that case, the energy flow to the C–H_r bond from the C–H_m bond is more efficient than the reverse energy flow; hence, the dissociation probability of the C–H_r bond becomes higher than that of C–H_m bond.

A similar E_T dependence is observed for the dissociation probabilities of the C–H_r and C–H_m bonds in the MP

+ O_2 reaction. In this case, the perturbations required to induce *intra*molecular energy transfer are expected to be more efficient because the mass of the collider (O_2) is slightly greater than that of N_2. Therefore, the dissociation probabilities of the C–H bonds are seen to be slightly higher than those in the MP + N_2 reaction at E_T values above 65,000 cm^{-1}, even though the differences are not large. Nevertheless, these bond dissociation probabilities in both the MP + N_2 and MP + O_2 collisions are similar to those in the toluene + N_2 and toluene + O_2 collisions[33] because the same colliders, with the same masses, are involved.

By contrast, the probabilities of C–H_r or C–H_m bond dissociation in the MP + N_2 and MP + O_2 systems are significantly higher than those of the toluene + H_2 or D_2 and a-CT + H_2 or D_2 systems.[34,35] In the latter collisions, the *inter*molecular perturbations are expected to be less efficient because a colliding molecule with lower mass than N_2 or O_2 is involved; hence, the dissociation probability of the C–H_r or C–H_m bond dissociation is low.

CONCLUSIONS

Herein, the inter-and intra-molecular energy transfer and C–H bond dissociations of methylpyrazine (MP) in collision with N_2 and O_2 at 300 K were studied using quasi-classical trajectory procedures. The reaction system consists of the interaction zone, where the colliding molecule interacts with both the methyl and ring C–H bonds (C–H_m and C–H_r), and the inner zone, which includes the various stretching and bending bond vibrations of MP. The results indicate that the energy loss by the vibrationally excited MP upon collision is not large, but increases slowly as the initial vibrational energy of the MP is increased from 5,000 to 30,000 cm^{-1}. With the further increase in initial vibrational energy above 30,000 cm^{-1}, however, the energy loss by MP decreases. Although the extent of energy loss by the excited MP is not large, the flow of intramolecular vibrational energy between the C–H bonds is highly efficient. The intermolecular energy transfer occurs mostly via vibration-to-translation ($V \rightarrow T$) and vibration-to-vibration ($V \rightarrow V$) transfers, whereas the vibration-to-rotation ($V \rightarrow R$) transfer is not significant. The $V \rightarrow T$ transfer exhibits a similar pattern in both systems as the initial vibrational energy of MP increases. However, the $V \rightarrow V$ energy transfer exhibits significantly different amounts and patterns between the two collision systems.

When the total energy content (E_T) is sufficiently high, either type of C–H bond can dissociate. When the initial vibrational energies of both C–H bonds are set below the dissociation threshold by the same amount, the dissociation probability of the C–H_m bond is higher than that of the C–H_r bond at E_T of less than 71,000 cm^{-1}, which can be interpreted as resulting from the intermolecular interaction. This is because the intermolecular perturbation of the C–H_m bond by the collision is more efficient than that of the C–H_r bond. At E_T values above 71,000 cm^{-1}, however, the dissociation probability of the C–H_r bond is higher than that of the C–H_m bond because the *intra*molecular energy flow to the C–H_r bond from the C–H_m bond is more efficient than the reverse energy flow. The dissociation probabilities of the C–H bonds are slightly higher in the collision with O_2 than in the collision with N_2. Nevertheless, the dissociation probabilities of the C–H bonds in both collisions are comparable with those observed in previous studies for toluene + N_2 and toluene + O_2 collisions.[23]

REFERENCES

1. Nakashima, N.; Yoshihara, K. *J. Chem. Phys.* **1983**, *79*, 2727.
2. Beck, K. M.; Gordon, R. J. *J. Chem. Phys.* **1987**, *87*, 5681.
3. Abel, B.; Herzog, B.; Hippler, H.; Troe, J. *J. Chem. Phys*. **1989**, *91*, 900.
4. Hippler, H.; Otto, B.; Troe, J. *Ber. Bunsen-Ges. Phys. Chem.* **1989**, *93*, 428.
5. Ma, J.; Liu, P.; Zhang, M.; Dai, H.-L. *J. Chem. Phys.* **2005**, *123*, 154306.
6. Hsu, H. C.; Tsai, M.-T.; Dyakov, Y. A.; Ni, C.-K. *Int. Rev. Phys. Chem.* **2012**, *31*, 201.
7. Ree, J.; Ko, K. C.; Kim, Y. H.; Shin, H. K. *J. Phys. Chem. B* **2021**, *125*, 874.
8. Zhang, R. M.; Xu, X.; Truhlar, D. G. *J. Phys. Chem. A* **2022**, *126*, 3006.
9. Yamada, Y.; Mikami, N.; Ebata, T. *Proc. Nat. Acad. Sci.* **2008**, *105*, 12690.
10. Ree, J.; Kim, Y. H.; Shin, H. K. *J. Chem. Phys*. **2022**, *156*, 204305.
11. Shin, H. K. *J. Phys. Chem. B* **2023**, *127*, 163.
12. Ree, J.; Ko, K. C.; Kim, Y. H.; Shin, H. K. *J. Phys. Chem. B* **2023**, *127*, 7276.
13. Pein, B. C.; Sun, Y.; Dlott, D. D. *J. Phys. Chem. A* **2013**, *117*, 6066.
14. Shin, H. K. *J. Phys. Chem. A* **2000**, *104*, 6699.
15. Khakoo, M. A.; Orton, D.; Hargreaves, R. *Phys. Rev. A* **2013**, *88*, 012705.
16. Kumar, R.; Nag, P.; Ranković, M.; Čurík, R.; Knížek, A.; Civiš, S.; Ferus, M.; Trnka, J.; Houfek, K.; Čížek, M.; Fedor, J. *J. Phys. Rev. A*. **2020**, *102*, 062822.
17. Lipkus, A. H.; Yuan, Q.; Lucas, K. A.; Funk, S. A.; Bartelt III, W. F.; Schenck, R. J.; Trippe, A. J. *J. Org. Chem.*

2008, *73*, 4443.
18. (a) Ree, J.; Chang, K. S.; Kim, Y. H.; Shin, H. K. *Bull. Kor. Chem. Soc.* **2003**, *24*, 1223; (b) Ree, J.; Kim, Y. H.; Shin, H. K. *Ibid.* **2005**, *26*, 1269.
19. (a) Hippler, H.; Troe, J.; Wendelken, H. J. *Chem. Phys. Lett.* **1981**, *84*, 257 (b) *J. Chem. Phys.* **1983**, *78*, 5351; *78*, 6709; *78*, 6718 (c) **1984**, *80*, 1853.
20. Toselli, B. M.; Brenner, J. D.; Yerram, M. L.; Chin, W. E.; King, K. D.; Barker, J. R. *J. Chem. Phys.* **1991**, *95*, 176.
21. (a)Bernshtein, V.; Oref, I. *J. Phys. Chem. A* **2006**, *110*, 8477. (b) *J. Phys. Chem. B* **2005**, *109*, 8310. (c) *J. Phys. Chem. A* **2006**, *110*, 1541.
22. Ree, J.; Oh, H.-G.; Lee, S. K.; Kim, Y. H. *Bull. Kor. Chem. Soc.* **2006**, *27*, 1641.
23. Ree, J.; Kim, Y. H.; Shin, H. K. *Bull. Kor. Chem. Soc.* **2013**, *34*, 1494.
24. Hirschfelder, J. O.; Curtiss, C. F.; Bird, R. B. *Molecular Theory of Gases and Liquids*; Wiley: New York, **1967**; see p. 168 for the combining laws, pp. 1110-1112 and 1212-1214 for *D* and *a*, respectively.
25. Zimmt, M. B.; Waldeck, D. H. *J. Phys. Chem. A* **2003**, *107*, 3580.
26. http://webbook.nist.gov/chemistry/name-ser.html (Accessed August 25, 2023).
27. Olney, T. N.; Cann, N. M.; Cooper, G.; Brion, C. E. *Chem. Phys.* **1997**, *223*, 59.
28. Gear, C. W. *Numerical Initial Value Problems in Ordinary Differential Equations*, Prentice-Hall, New York, **1971**.
29. MATH/LIBRARY; *Fortran Subroutines for Mathematical Applications*; IMSL; Houston, **1989**; p. 640.
30. Ree, J.; Kim, Y. H.; Shin, H. K. *J. Chem. Phys.* **2002**, *116*, 4858.
31. Wright, S. M. A.; Sims, I. R.; Smith, I. W. M. *J. Phys. Chem. A* **2000**, *104*, 10347.
32. Lee, S.-J.; Ree, J. *Bull. Kor. Chem. Soc.* **2019**, *40*, 882.
33. Lim, K. F. *J. Chem. Phys.* **1994**, *101*, 8756.
34. Ree, J.; Kim, Y. H.; Shin, H. K. *Bull. Kor. Chem. Soc.* **2013**, *34*, 3641.
35. Lee, S. K.; Ree, J. *Bull. Kor. Chem. Soc.* **2021**, *42*, 773.